Energy, Mines and Resources Canada | Énergie, Mines et Ressources Canada

CANMET

Canada Centre for Mineral and Energy Technology | Centre canadien de la technologie des minéraux et de l'énergie

PILOT-SCALE COMBUSTION STUDIES OF COAL-WATER FUELS: THE CANADIAN R & D PROGRAM

K.V. Thambimuthu, H. Whaley and C.E. Capes

For Presentation at 2nd European Conference on Coal Liquid Mixtures, London, England, Sept. 16-18, 1985 and submitted to the Institution of Chemical Engineers (U.K.) Symposium Series No. 95, 1985.

ENERGY RESEARCH PROGRAM
ENERGY RESEARCH LABORATORIES
DIVISION REPORT ERP/ERL 85-08(OPJ)

PILOT-SCALE COMBUSTION STUDIES OF COAL-WATER FUELS: THE CANADIAN R & D PROGRAM

by

K.V. Thambimuthu*, H. Whaley* and C.E. Capes**

ABSTRACT

Pilot-scale studies undertaken as part of the Canadian coal-water fuels program are described. These studies included a comparison of the combustion and heat transfer characteristics of a domestic coal-water fuel, pulverized coal and heavy fuel oil, and combustion tests to evaluate the performance of a new wear resistant atomizer that was developed for coal-water fuels. Detailed results from these studies and their relevance to industrial and utility processes are described.

---

*Research Scientists, Combustion and Carbonization Research Laboratory, Energy Research Laboratories, CANMET, Energy, Mines and Resources Canada, Ottawa, K1A 0G1.

**Head, Chemical Engineering Section, Division of Chemistry, National Research Council of Canada, Ottawa K1A 0R9.

ESSAIS DE COMBUSTION À L'ÉCHELLE PILOTE DE MÉLANGES CHARBON-EAU: LE PROGRAMME CANADIEN R-D

par

K.V. Thambimuthu*, H. Whaley* et C.E. Capes**

RÉSUMÉ

Le rapport présente des essais de combustion à l'échelle pilote menés dans le cadre du programme canadien de recherche sur la combustion de mélanges charbon-eau. Les activités de recherche portaient également sur la comparaison des caractéristiques de combustion et de transfert de chaleur d'un combustible domestique charbon-eau, de charbon pulvérisé, de fuel lourd et comprenaient des essais de combustion visant à évaluer la résistance à l'usure d'un nouveau pulvérisateur mis au point pour la combustion des mélanges charbon-eau. Le rapport présente également le détail des résultats de ces essais et leur portée sur les procédés de combustion auxilliaire et industrielle.

---

*Chercheurs scientifiques, Laboratoire de recherche sur la combustion et la carbonisation, Laboratoires de recherche sur l'énergie, CANMET, Énergie, Mines et Ressources Canada, Ottawa, K1A OG1.

**Chef, Section du génie chimique, Division de la chimie, Conseil national de recherche du Canada, Ottawa K1A OR9

CONTENTS

TABLES

FIGURES

Contents (Cont'd)

FIGURES

INTRODUCTION

The Federal Government of Canada [Energy, Mines and Resources (EMR)] has identified coal-water fuels (CWF) as a priority, and has directed substantial efforts towards the development of CWF technology. Major initiatives have included the construction of a 4 t/h CWF preparation plant in Sydney, Nova Scotia, the development of CWF fuel burners and the demonstration of CWF combustion in two utility boilers [10 MW(e) front wall fired and a 22 MW(e) corner fired] in Chatham, New Brunswick (1). It is expected that the CWF demonstration in these coal-designed boilers will be followed by the scale-up and demonstration of CWF technology in oil-designed utility boilers in the 20-150 MW(e) capacity range (1,2). As a spin-off from these initiatives, a number of industrial demonstrations and applications of CWF in cement kilns, iron ore induration furnaces and nickel smelters are also being pursued (2).

In their role as federal government research agencies, both the Canada Centre for Mineral and Energy Technology (CANMET) and the National Research Council of Canada (NRCC) are engaged in R & D activities in support of the above developments. The work reported in this paper describes some of the pilot-scale studies undertaken by contract and in-house research to address the following key issues:

i) Assessment of the combustion and heat transfer characteristics of CWF, pulverized coal and heavy fuel oil in order to delineate critical hardware and fuel-related parameters relevant to CWF substitution.
ii) Combustion tests for a performance evaluation of a prototype wear-resistant ceramic tip atomizer developed by NRCC.

COMPARATIVE EVALUATION OF THE COMBUSTION AND HEAT TRANSFER CHARACTERISTICS OF CWF, PULVERIZED COAL AND HEAVY FUEL OIL

EXPERIMENTAL

The experimental study on the combustion and heat transfer characteristics of the domestic CWF, the parent pulverized coal (Lingan Coal; Cape Breton Harbour Seam) and No. 6 fuel oil was carried out in a pilot-scale flame tunnel furnace at CANMET's Energy Research Laboratories. A schematic of the flame tunnel is shown in Fig. 1. The main chamber of the flame tunnel is made

up of 28 cylindrical calorimetric sections, 1 m I.D. with a total length of 4.2 m. Sealed water-cooled doors with circular probe holes are located in the gaps of the cooling segments. The probe holes provide radial and axial access to the furnace environment for the measurement of flame properties. The main furnace chamber is preceded by a 0.83 m I.D., 1 m long refractory-lined adiabatic pre-chamber. The burner quarl used in the study was a 0.54 m deep, 2.3° half angle, divergent conical refractory quarl with a 0.18 m inlet throat and a 0.23 m exit hole. The burner installed at the inlet of the quarl was a dual fuel gas/oil burner. The fuel nozzle assemblies shown in Fig. 2, 3 and 4 were specially adapted for CWF, heavy oil and pulverized coal firing. Flue gases leave the flame tunnel via a converging section and a 0.3 m square duct connected to a water cooled heat exchanger with an induced draft fan to the stack. During normal operation, a balanced draft is maintained at the furnace exit to minimize in-leakage of ambient air into the furnace chamber.

Aside from routine measurements of input and output variables to monitor furnace performance, the following parameters were also measured: in-flame gas temperatures, axial distributions of the total and cooling load heat fluxes, in-flame and exit gas compositions and the total flue particulate loadings. Details of the flame probes used for the temperature measurement, total heat flux measurement and in-flame gas sampling have been described previously (3). In addition, particle size distributions were analyzed by a Coulter Counter and small samples of the solids were analyzed by scanning electron microscopy for qualitative determinations of the particle morphology.

OPERATING CONDITIONS AND FUEL PROPERTIES

The input and operating conditions of the flame tunnel are summarized in Table 1. The fuels were fired at a nominal thermal input of 0.45 MW, with excursions in the firing rate between 0.416 and 0.483 MW noted for the CWF and pulverized coal. For each fuel, three tests were carried out at 1, 3 and 5% excess O_2 concentrations in the flue gas in order to investigate the effect of excess air and residence time on fuel conversion. The refractory-lined burner quarl and pre-chamber provided a 1.54 m long adiabatic zone and greatly influenced initial temperatures and the ignition stability of the flames (see below). The coolant flowrates in the furnace segments were maintained at identical values for all test runs so that the differences in the heat flux profiles between fuels were determined by the combustion and heat transfer characteristics of the flames.

The mass ratios of the atomizing air to fuel flowrates, shown in Table 1, are high, being significantly larger than the 0.2-0.4 ratio that is desirable for an optimized fuel nozzle (4). The fuel nozzle assembly for heavy oil was initially selected for both CWF and heavy oil firing (Fig. 3). However, a number of difficulties were experienced with CWF atomization and ignition using this nozzle, and the internally atomized nozzle shown in Fig. 2 was chosen as a replacement. The dimensions selected for the fuel and air outlet diameters and the final dispersion gaps in the internally and externally atomized nozzles were optimized values necessary to produce symmetrical stable flames, and without fuel dripping or coking. As noted above, these dimensions did not provide economical atomizing air utilization. The high atomization air flowrates had a significant influence on axial fuel-air mixing, affecting combustion as noted later. Significant erosion was noted for the CWF nozzle, and overall wear data are summarized in Fig. 2.

Tables 2 and 3 summarize data on the physical and chemical properties of the fuels. The CWF had an average composition of 70 wt % coal, 29 wt % water and up to 1 wt % proprietary surfactant additives, viscosity modifiers and an algicide. Viscosity data supplied by the fuel manufacturer show that the fuel is thixotropic. The CWF had excellent handling characteristics with very little evidence of solids separation or settling, but tended to solidify quickly on air exposed surfaces when splashed or spilled in thin stagnant pools. The particle size distribution in the CWF, with size data expressed as the volume equivalent spherical diameter is shown in Table 2 and Fig. 13. The coal particles in the CWF had a mean diameter of 36 μm with 86% less than 75 μm. For the pulverized coal, the volume mean diameters were 25 μm (99% below 75 μm), 28 μm (96.5% below 75 μm) and 38 μm (89% below 75 μm) for runs PC1, PC2 and PC3 respectively. Ultimate and proximate analyses show that the coal and ash composition are very nearly identical for the CWF and pulverized coal, except for a 60% reduction in the ash content in the CWF.

IGNITION STABILITY AND FLAME TYPE

The most significant early problem encountered in the experimental trials was achieving stable ignition of the CWF. Early experience with a wide divergent quarl, in which a flame could only be stabilized with gas support, showed that significant energy feedback to the fuel spray was required for moisture evaporation, heating and devolatilization of the coal particles

(5,6). In order to provide this energy, the narrow quarl described above was adopted. Improved radiant and convective heat transfer, promoted by the hot refractory surfaces located close to and concentric with the fuel spray, improved ignition stability, and flame propagation, producing CWF flames that were self-sustaining after a brief preheat period with gas support. Pulverized coal and No. 6 oil were fired using the same quarl. This was necessary in order to obtain flames with similar mixing patterns that would permit a valid comparative combustion evaluation of the fuels.

The ducted quarl, secondary airflow distribution pattern, and the fuel nozzles produced confined jet turbulent diffusion flames, with combustion and heat transfer properties that are determined by axial mixing gradients between the fuel jet and the secondary combustion airflow (4). Axial mixing arises from momentum exchange between the fuel jet and the secondary airflow caused by frictional entrainment of fluid across the boundaries of the jet. In the ducted quarl, availability of the secondary airflow less than that which the jet can entrain promotes an axial recirculation eddy within the quarl (4). The recirculation eddy transfers hot gas back to the core of the flame. The size, strength and axial position of the recirculation eddy from the burner depends on the initial momentum of the fuel jet, its rate of divergence (initially dependent on nozzle geometry and the method of fuel dispersion) and the amount of secondary air available for flow entrainment. These factors show that axial fuel-air mixing is initially more rapid for the pulverized coal flames (large nozzle inlet with a high air-fuel mass ratio), intermediate for CWF and lowest for No. 6 oil. The latter is because external atomization of oil produces a more confined fuel jet with slow radial dispersion characteristics.

Visual inspection of the flames showed that the pulverized coal and CWF flames expanded radially filling the discharge hole of the quarl, while the oil flames were of a smaller diameter. From these observations, it was concluded that the internal recirculation eddy was not formed for the oil flames resulting in some discharge of the secondary airflow into the adiabatic pre-chamber. For the coal flames, the convective heat transfer of recirculated hot gas within the quarl and radiant heat transfer from the refractory walls improved the ignition stability as noted earlier. Besides flow recirculation in the quarl, flame discharge into the larger furnace chamber also induced a secondary recirculation flow, due to frictional entrainment caused by

the large radial and axial velocity gradients within the flame envelope. The secondary recirculation eddies were external and located in an area between the flame envelope and the furnace walls, extending over an axial distance from the quarl exit to the flame tip (visually observed flame lengths of 2-2.5 m). Evidence confirming the presence of the secondary recirculation zone and its impact on the measured flame properties are described later.

GAS TEMPERATURES

Radial temperature profiles for the 1% excess O_2 runs measured at the 1.87 and 2.92 m axial stations are shown in Fig. 5 and 6. At the 1.87 m station the temperature profiles are very nearly identical for No. 6 oil and pulverized coal, but are lower by as much as 200°C for CWF. A similar trend is obvious at the 2.92 m station but with slightly lower temperatures for pulverized coal when compared with oil. The radial temperature profiles at the 1.87 m station located between the quarl exit and the flame tip are parabolic, with a 300-400°C temperature drop between the furnace axis and walls. The large temperature gradients are caused in part by the high temperatures within the flame envelope and the recirculation flow outside that transfers low temperature gases from a downstream to an upstream location in the furnace. At the 2.92 m axial station, which is beyond the visually measured flame tip, the temperature profiles are of a plug flow type with the net forward movement of gases in the furnace.

Peak temperatures at the furnace axis plotted as a function of the axial distance from the burner are shown in Fig. 7. The centreline temperatures for all three fuels show a general trend of decreasing temperatures with increasing axial distance, but appear to approach limiting values at positions close to the burner and at the flue duct. In the former, the high limiting temperatures represent the maximum flame temperatures achieved with fuel combustion in the adiabatic refractory zones in the furnace, whereas the lower limit is caused by the absence of a cooling load at the flue exit section. At intermediate positions, the temperatures drop by gas dilution from flow recirculation and by heat loss to the furnace cooling loops. The axial temperature profiles show the highest measured values for No. 6 oil, intermediate for pulverized coal, and lowest for CWF (200°C < No. 6 oil). Highest temperatures measured for the oil stem from the high fuel conversion efficiencies, and the accompanying high heat release rates per unit volume of gas

caused by the lower stoichiometric combustion air requirements when compared to coal. For pulverized coal, lower fuel conversion efficiencies and the larger combustion gas volumes produced marginally lower gas temperatures when compared with oil. Applying similar arguments to the CWF for which the fuel reactivity is identical to pulverized coal, it can be seen that the lowest gas temperatures are caused in part by the energy initially required to evaporate the water in the fuel. From these observations, it appears that the lower flame temperatures for CWF results in a penalty on fuel conversion efficiences (see below) in addition to the estimated 3% overall heat loss incurred by the water present in the fuel.

HEAT FLUX

Figure 8 shows the axial distribution of the total heat flux for the 1% excess O_2 runs measured by conductivity plug type heat flux meters (3). The axial distribution of the heat flux removed by the furnace cooling circuits for the same conditions are shown in Fig. 9. The total heat flux and the heat flux removed by the cooling circuits are the sum of the radiant and convective heat fluxes, but the radiant component in the former is the radiant energy absorbed by a black body ($\varepsilon=1$), whereas the radiant component in the latter is the energy absorbed by a real surface ($\varepsilon<1$). Similarly, the convective driving force measured by the heat flux probe does not include the cooling liquid boundary layers which are barriers to heat transfer. Hence, the total heat flux represents the potential driving force available for energy transfer to the surrounding cylindrical heat transfer surface, while the cooling load heat flux is the actual energy absorbed by the surface.

The total and cooling load heat flux profiles decrease exponentially with increasing axial distance from the burner with lowest measured values for CWF. Besides the clearly identifiable trend for CWF, values of the total heat flux measured at four axial positions are not sufficiently acccurate to delineate relative trends between the oil and pulvervized coal. Examination of the axial cooling heat fluxes (Fig. 9) shows that the heat fluxes are highest for oil, intermediate for pulverized coal and lowest for CWF closest to the burner, with a switch in the relative positions for oil and pulverized coal at locations more than 3 m from the burner. A comparison with the axial distribution of centreline temperatures (Fig. 7) shows that at positions close to the burner, the gas temperatures and the cooling load heat fluxes maintain

identical trends relative to fuel type. With the dominant influence of temperature on radiant heat transfer and the higher flame emissivity expected for an oil flame, due to the presence of fine soot particles, the higher cooling load heat flux for No. 6 oil is caused by higher radiant heat transfer to the cooling circuits at positions close to the burner. With more complete radial mixing of the gases beyond the flame tip and the higher gas throughputs in the furnace relative to oil, the cooling load heat flux is higher for pulverized coal due to higher convective heat transfer to the cooling circuits. In all cases, lower temperatures and gas throughputs for CWF produced lowest measured values of the cooling load heat flux through lower radiant and convective heat transfer. With sufficiently detailed measurements, the same trends should be apparent for the total heat flux due to the similarities noted in the component heat flux terms.

GAS COMPOSITIONS

Radial profiles of the in-flame O_2 and NO_x concentrations for the 1% excess O_2 runs measured at the 1.26 m axial station are shown in Fig. 10 and 11. The concentration profiles are symmetrical about the furnace axis with characteristic minima or maxima measured within the flame envelope. Similar profiles were measured for the in-flame CO_2 and CO concentrations. As expected, the in-flame CO_2 profiles were usually exact mirror images of the corresponding O_2 profiles, i.e., with a characteristic minimum when the O_2 profile is at a maximum and vice versa. The CO concentration profiles in all cases peaked at the flame axis. With increasing excess O_2 in the flue gas, or with increasing axial distance along the flame, the radial gas concentration profiles maintained identical shapes, albeit at different equilibrium gas concentrations.

As shown in Fig. 10, the O_2 profiles for CWF and pulverized coal peak at the flame axis, whereas the corresponding curve for No. 6 oil shows a characteristic minimum. The difference in O_2 profiles for the coal and oil flames stem from characteristic differences in the axial fuel-air mixing patterns and the reactivity of the fuels. The formation of internal and external recirculation eddies for the coal flames causes flow recirculation and mixing of gases outside the flame envelope which originate from different axial locations within the flame envelope. The mean O_2 concentration outside the flame envelope is thus lower, and peaks within the flame envelope because the gas-

solids reactions with the coal particles are not sufficiently rapid to cause a significant radial decay in the in-flame O_2 concentration. For the oil flame on the other hand, discharge of the secondary combustion airflow into the main furnace chamber and mixing of this higher O_2 concentration airflow with spent gases recirculated by the secondary recirculation eddies, results in a higher measured O_2 concentration outside the flame envelope. With the gas phase combustion of a more highly volatile and reactive fuel within the flame envelope, the O_2 concentration drops to a minimum at the flame axis because the flame temperatures are highest at that location (Fig. 5, 6 and 7).

Figure 11 shows that the high flame temperatures at the furnace axis also cause a peak in the in-flame NO_x radial profiles. NO_x in the flame originates from the high temperature fixation of atmospheric N (thermal NO_x) and from the oxidation of N chemically bound in the fuel (fuel NO_x). Experimental studies on NO_x formation in pulverized coal flames show that at least 70% of the total concentration formed originates from fuel N (7). Fuel compositions in Tables 2 and 3 show that the fuel N content is lowest for No. 6 oil and highest for CWF, so that a similar trend should be apparent for the measured NO_x gas concentrations. The data in Fig. 11 are in good agreement with the expected trend for oil, but show lower concentrations for CWF relative to pulverized coal. However, the energy consumed by water evaporation for CWF produced lower flame temperatures, so that lower fuel and thermal NO_x formation may be expected in comparison to pulverized coal. NO_x concentrations in the flue gas shown in Table 1, maintain an identical trend with fuel type as that noted for the in-flame NO_x. With increasing excess air, the volume concentrations in the flue gas go through a characteristic maximum at intermediate excess air levels. This trend is equivalent to combustion air staging, which at low excess air diminishes NO_x production, increases with excess air and decreases once again with volume dilution and lower combustion temperatures at high excess air (7).

FUEL BURNOUT, FLUE PARTICULATES AND FURNACE DEPOSITS

Figure 12 shows a plot of the fractional fuel burnout efficiency, Cx, versus the excess O_2 in the flue gas. The fractional fuel burnout efficiencies for the oil runs were calculated from a carbon balance on the fuel, with measured levels of the soot particles in the flue gas taken as the total unburnt carbon. For CWF and pulverized coal, the burnout efficiency was calcu-

lated by an ash tracing technique, with the unburnt fuel taken as the complementary weight fraction of the ash in the flue particulates (8).

The results in Fig. 12 show that the fuel burnout efficiencies are highest for oil, marginally less for pulverized coal and lowest for the CWF. The burnout efficiencies for oil increase with increasing excess oxygen in the flue (see Table 1), as may be expected with improved fuel conversion at a higher oxidant concentration in the flame. The corresponding results for CWF and pulverized coal show a similar trend at low and intermediate excess air, but decrease at high excess air. The lower measured efficiencies for pulverized coal and CWF, despite improved axial mixing between the fuel and oxidant relative to oil, are caused by the slower mass transfer and chemical rate limited gas-solids reactions that require a longer residence time in the furnace for good carbon burnout (9). The crucial effect of the solids residence time is also demonstrated in the measured fuel burnout efficiencies at high excess air for the coal, which despite the higher oxidant concentration, decreases because of the higher gas volume throughput and hence a shorter time spent by the coal particles in the reaction environment. Compared with pulverized coal, the lower flame and gas temperatures for CWF are mainly responsible for poorer fuel burnout efficiencies.

Figures 13 and 14 show the particle size distributions of the flue solids and the coal in the fuels for the 1% excess O_2 CWF and pulverized coal runs. The flue ash particles have a smaller volume mean diameter than the coal particles in the fuel due to a pronounced reduction in the volume concentration of coarse particles in the particle size distribution. The reduction in the mean diameter of flue particulates, despite the high free swelling index of the coal (Table 2), is caused by the size reduction with carbon burnout, particle attrition and deposition of some large particles in the furnace.

SEM analyses of the flue particulates showed a large population of cenosphere type char and ash particles with a high bulk concentration of unburnt carbon (Table 1). The solids from pulverized coal combustion were highly fused cenospheres due to higher flame temperatures experienced by the particles. A porous skeletal ash matrix within the particles and a highly porous surface with a large number of small blow holes were observed. Some of the cenospheres from CWF combustion had similar characteristics, but a major proportion of the particles were cenospheres with a small number of

large blow holes with empty cavities within the particles. A number of these particles were oblate and appeared to have been formed by the fusion of two or more coal particles. A significant amount of broken cenospheres exposing large internal cavities and smaller pieces from these cenospheres were also evident. The presence of the cenosphere agglomerates showed that fuel agglomeration had taken place during atomization and combustion of the CWF.

In order to characterize CWF agglomeration, corresponding samples of the pre-chamber, middle and rear furnace deposits were subjected to similar analyses. The particle size distribution of the pre-chamber deposits in Fig. 13 shows a marginally smaller volume mean diameter than that for the coal particles in the fuel. However, below 25 μm, the size distribution of the pre-chamber deposits are coarser than the fine coal and ash particles in the fuel. A large number of fine ash particles are expected because of fuel beneficiation by water flotation. Attempts to analyze the particle size distribution of the middle and rear furnace deposits met with limited success, due to rapid plugging of the aperture tube in the Coulter Counter by some of the larger particle agglomerates in these deposits. The SEM analysis of the pre-chamber deposits showed a very large population of very fine, irregular, reddish brown ash particles, the majority of which appeared to have bonded together into medium and large clusters of multi-particle agglomerates. The middle and rear furnace deposits were mainly char particles with unburnt carbon 5-10 wt % higher than the carbon in the flue particulates. Most of the char particles were agglomerates that appear to have originated from a number of coal particles in large fuel droplets that have fused together to form single hollow cenospheres during the heating, devolatilization and ignition stages of fuel combustion. Some of these cenospheres were very large with particle sizes at least 300 μm in diameter. It is clear from these observations that most of these particles were dropped in the furnace by inertial separation from the gas flow. Other studies on CWF combustion have also identified similar deposits and show that atomization is critical for good CWF combustion (5,8). In addition to the lower flame and gas temperatures caused by the water present in the fuel, the agglomerates formed also affected carbon burnout through a slower mass transfer limited reaction rate expected for larger char particles (9).

Some deposition in the furnace was also noted for the pulverized coal which raises the possibility that the fuel burnout efficiencies reported in

Fig. 12 may be suspect, because of the unaccountability of the carbon in these deposits. For verification, carbon burnout was calculated using measured values of the CO_2 concentration in the flue gas. These values ranged from 2% lower for oil, 2% lower and 6.3% higher for pulverized coal and 10% higher for CWF when compared with the ash tracing values. However, the calculation requires very accurate measurements of fuel and air throughputs with no leakage of gas in or out of the furnace chamber. In any event, the carbon burnout efficiencies measured in these pilot-scale tests should only be used as an indication of relative trends. Larger scale equipment, through the decreased surface area to volume ratio and higher heat release rates would improve the carbon conversion efficiencies.

CWF AND HEAVY OIL COMBUSTION TESTS WITH THE NRCC ATOMIZER

Combustion tests to evaluate the performance of the prototype NRCC ceramic tip atomizer were undertaken in a pilot-scale flame tunnel furnace at the Centre of Energy Studies (CES), Technical University of Nova Scotia. The CES flame tunnel has a 1.17 m I.D. and 3.0 m long combustion chamber made up of five water cooled segments with access holes for flame probing. The bottom of the furnace has a refractory lined hearth covering 45% of the internal surface area. The flame tunnel is equipped with a modified Babcock-Duiker swirl register and a divergent 35° half angle refractory quarl. The combustion air flow to the furnace is admitted into a plenum and enters the quarl through the swirl register which has adjustable swirl vanes for tangential air entry, and adjustable concentric openings in the back face of the register for axial air entry. The gases leave the furnace through a concentric 0.4 m I.D. duct at the end of the furnace chamber. Combustion air is delivered by a forced draft fan with indirect steam heating and/or direct propane firing for air preheating. The exit gas is evacuated by an induced draft fan connected to the stack with ambient air entry through a temperature controlled damper for flow cooling. The furnace is operated with a balanced draft at the furnace exit. The gas sampling and flame probing equipment used in these tests were essentially identical to those described earlier.

The NRCC atomizer is a conical spray twin fluid atomizer with an outer annular fuel stream and an inner axial atomizing fluid stream. The atomizing fluid emerges via tangential slots in a stem holding a ceramic cone and flows outwards in a conical stream at an angle to the nozzle axis determined by the included angle of the spray cone. The annular fuel stream goes through a 90° change in its flow direction, flows horizontally towards the spray cone where the diverging conical air stream impinges on the fuel sheath. A ceramic wear ring which forms the upper surface of the fuel sheath has an angled hole in the centre which matches the spray angle of the ceramic cone. The gap between the wear ring and cone over the thickness of the wear ring forms the mixing chamber and exit gap from the atomizer. The wear ring and cone are changeable parts for the alteration of the fuel spray angle. The thickness of the horizontal fuel sheath can be adjusted by spacers of different thicknesses to match fuel rheology to atomization and to control fuel throughputs at the desired pressure. Similarly, the vertical position of the

stem holding the cone can also be adjusted for alteration of the atomizing medium and final dispersion gaps, and this provides an independent control of the atomizing medium throughput and pressure. The gun assembly below the spray head described above is equipped with a heat exchanger for fuel preheating or cooling depending on the application desired. A thermocouple inserted in the same assembly is used to monitor the fuel temperature. At the time of writing, a schematic diagram of the NRCC atomizer could not be included for proprietary reasons.

Table 4 summarizes the test conditions in the furnace for the CWF and No. 6 fuel oil runs. The fuels were fired at a nominal throughput of 1.8 MW(th) with a 5% excess O_2 concentration in the flue gas. Both air and steam atomization were employed. The furnace cooling load of 0.81 MW(th) maintained in these tests correspond to 45% of the thermal input. The atomizing medium to fuel mass ratios were between 0.23-0.33 for the CWF and 0.41-0.42 for heavy oil and were comparable to those levels desired for an optimized fuel atomizer. Fuel compositions and properties were not significantly different from those reported in Tables 2 and 3. When firing heavy oil the fuel was heated to a temperature of 104°C. Cooling to maintain a temperature of 30-31°C was used for the CWF. In all cases, the combustion air to the furnace was heated to maintain temperatures between 230-260°C.

Swirling combustion air jets are used to promote mixing between the fuel stream and combustion airflow and to improve the ignition stability and combustion intensity of flames (4). When a rotating motion is imparted to the combustion airflow upstream of the burner quarl, the fluid flow emerging from the quarl has tangential, axial and radial velocity components. The tangential velocity spins the airflow outwards on emergence from the burner quarl, and induces a large internal torroidal vortex reverse flow region at the flow axis. In addition, the velocity gradients in the swirling air jet also create an external recirculation zone between the jet and the constraining walls of the burner chamber. The strength and size of the internal recirculation zone (IRZ) is, amongst other factors, mainly dependent on the angle of divergence of the burner quarl and the swirl numbers (the ratio of the tangential and axial momentum of the combustion airflow). At intermediate or high swirl numbers, the combustion airflow is stably attached to the divergent walls of the quarl, producing highly stable flames with fuel ignition close to the exit of the fuel nozzle due to the reverse flow of hot combustion products promoted

within the IRZ. This flow pattern enables close matching of the zones of high turbulence intensity and mixing at the interface of the IRZ, with those of high fuel concentration (the spray trajectory), producing short flames with a high combustion intensity.

Figures 15 and 16 show the flame flow boundary maps measured for the CWF and heavy oil tests with the NRCC atomizer. The experimental points of the forward and reverse flow regions (of zero axial velocity) were measured using and oxy-acetylene flame boundary probe for the CWF and a Hubbard probe for the oil. These measured points, together with the loci of the in-flame peak radial temperatures in the burner near-field region, show flame aerodynamic patterns identical to those described above. For the quarl, furnace geometry and spray momentum of the NRCC atomizer used in these tests, a 50° and 60° spray angle for CWF and heavy oil respectively were found necessary to produce the shortest flames with the highest combustion intensity. Fuel ignition occurred close to the atomizer exit with flow recirculation and location of the spray trajectory within the IRZ. For CWF, this recirculation flow provided the convective heat flux necessary for moisture evaporation, ignition and devolatilization of the coal particles. The combination of these optimized mixing patterns and the combustion air preheat also permitted easy light-off of the CWF in a cold furnace, together with a short period of propane support.

The loci of the peak radial in-flame temperatures, which corresponded to the fuel rich zones, show a diverging trajectory in the near field region with flow divergence of the swirling jet. Further down the furnace, re-convergence of the gas flow towards the exit flue duct caused a fuel rich zone to develop on the flow axis, with peak temperatures measured at that location. With the flow convergence, the axial profiles of the centreline temperatures in Fig. 17 and 18 provide a rough guide of the relative performance of the fuels. In the near field region, lower axial temperatures for CWF suggest lower combustion efficiencies and heat flux profiles relative to oil, but increase at the back-end of the furnace due to the longer residence time required for char combustion. For CWF and heavy oil, steam atomization produced lower axial temperatures, but the data for the radial temperature profiles at positions between $x/L = 0.17$ and $x/L = 0.53$ showed higher measured peak temperatures relative to the air atomized runs. Hence, the average fuel burnout efficiencies reported in Table 4 show no significant change with the type of

fluid used for fuel atomization. Good atomization of the CWF also produced fuel burnout efficiencies in the high nineties and were comparable to the corresponding oil values (Table 4). No wear was detected in the NRCC atomizer throughout the estimated 200 h total duration of the tests with CWF.

RELEVANCE OF THE WORK TO INDUSTRIAL AND UTILITY PROCESSES

The turbulent co-axial diffusion flames described earlier were designed to simulate flames encountered in industrial kilns and ore processing furnaces. Attempts to disperse the CWF by a single hole externally mixed oil atomizer used in iron ore induration machine burners showed poor fuel dispersion and ignition characteristics, while a substitute internally mixed oil nozzle showed significant erosion wear with a marginal improvement in fuel atomization. The laboratory work also showed that the water present in the fuel caused some difficulties with fuel ignition, requiring high convective and radiant heat fluxes to the core of the flame to sustain a stable and well ignited CWF flame. In the absence of combustion air swirl to promote axial fuel-air mixing, the convective and radiant heat fluxes are provided by a fuel jet-assisted recirculation flow in a ducted quarl located close to and concentric with the fuel spray.

In field trials on a 0.6-3.5 MW(th) iron ore induration machine burner, high preheat temperatures (800-900°C) of the co-axial combustion air stream was sufficient to ensure rapid moisture evaporation, devolatilization and ignition of the coal particles in the fuel spray (10). However, the NRCC atomizer used in these field trials showed that a CWF atomizer with good fuel dispersion characteristics, a high spray momentum and a wide spray angle, which is sufficient to promote rapid axial fuel-air mixing, was necessary in order to achieve fuel combustion within the refractory zone of the induration machine burner (10).

For industrial process burners with fuel jet-assisted mixing, the foregoing example shows that the ignition stability of CWF, the degree of combustion air preheat, atomization characteristics, spray momentum and angle are the critical factors affecting heavy oil substitution by CWF. However, the comparative evaluation of fuels in the laboratory work shows that a thermal penalty is incurred by the water present in the fuel. Similarly, carbon burnout may be lower, and would depend on the actual process gas temperatures and the residence time of the char particles in the furnace.

Combustion tests with the prototype NRCC atomizer in a swirling combustion air jet produced turbulent diffusion flames typical of some utility boiler burners. Good CWF atomization, matching of the spray momentum and angles to direct the fuel spray trajectory into a zone of high turbulence intensity and mixing at the interface of the IRZ and the swirling combuston airflow, produced short intense flames with good carbon burnout. Flow recirculation of hot gases in the IRZ greatly aided the ignition stability of CWF, but the carbon burnout was lower relative to heavy fuel oil because of the longer residence time required for the complete combustion of char particles. In marked contrast to the laboratory tests comparing the relative performance of CWF, heavy fuel oil and pulverized coal, better atomization of the CWF produced higher gas temperatures in the back-end of the furnace relative to the temperatures measured for heavy fuel oil. These higher gas temperatures show that the combustion and heat transfer characteristics of CWF would be similar to that expected for pulverized coal burning in a utility boiler, with some differences arising in the front-end of the boiler due to the lower flame temperatures caused by the water present in the fuel. The improved combustion performance of CWF in the tests with the NRCC atomizer, with a rated firing capacity of 0.6-3.5 MW(th) and no erosion wear, also showed it to be an ideal candidate for an application as a fuel atomizer in utility plant burners. Work is now proceeding on the development and testing of two 12 MW(th) atomizers at the Chatham generating station in New Brunswick. This work is being undertaken in preparation for the CWF demonstration trials in an oil-designed utility boiler in Charlottetown, Prince Edward Island (2).

ACKNOWLEDGEMENTS

The authors wish to express their gratitude to the Manager, G.K. Lee for his many helpful comments, and to the staff of the Industrial Combustion Processes Section, Combustion and Carbonization Research Laboratory, Energy Research Laboratories, CANMET for carrying out the pilot-scale experiments described in the early sections of this paper. Significant contributions from W. Thayer and A. Bennet of the National Research Council of Canada, who are deeply involved in the NRCC atomizer development, is also gratefully acknowledged. Lastly, the authors wish to express their thanks to Dr. M.J. Pegg and staff at the Centre for Energy Studies, Technical University of Nova Soctia for the work performed in the combustion tests with the NRCC atomizer.

REFERENCES

1. Read, P.J. and Whaley, H. "Status report on the Canadian coal-liquid mixture program"; I. Chem. E. Symposium Series, No. 85, p. 259-268, 1983.

2. Read, P.J., Whaley, H. and Rankin, D. "Developments in Canada's coal liquid fuels program" (in preparation); I. Chem. E. Symposium Series, No. 95, 1985.

3. Chedaille, J. and Braud, Y. "Measurements in flames - Volume 1"; Edward Arnold, London, U.K., 1972.

4. Beer, J.M. and Chigier, N.A. "Combustion aerodynamics"; Applied Science Publishers Ltd., London, U.K., 1972.

5. Beer, J.M. et al. "The combustion, heat transfer, pollutant emission and ash deposition characterisitics of concentrated coal-water slurries"; American Flame Research Committee, Fall Symposium, Akron, Ohio, Oct. 4-6, 1983.

6. Pourkashanian, M. and Williams, A. "The combustion of coal-water slurries"; I. Chem. E. Symposium Series, No. 85, p. 149-169, 1983.

7. Lee, G.K., Whaley, H. and Heap, M.P. "The control of NO_x and SO_x emissions from conventional pulverized coal flames: The Canadian program"; Amer Soc Mech Eng Joint Power Conference, October 1-4, Toronto, Canada, Paper No. 84-JPGC-FU-16, 1984.

8. Bortz, S., Engelberts, E.D. and Schreier, W. "A study of the combustion characteristics of a number of coal-water slurries"; Sixth International Symposium on Coal Slurry Combustion & Technology, Orlando, Florida, p. 710-730, June, 1984.

9. Field, M.A. et al. "Combustion of pulverized coal", British Coal Utilization Research Association, Leatherhead, U.K., 1967.

10. Thambimuthu, K.V., Personal Communication, Energy Research Laboratories, CANMET, Energy, Mines and Resources Canada, Ottawa, Canada, 1984.

Table 1 - Furnace operating conditions: CWF, pulverized coal and No. 6 oil

Fuel	Coal water fuel			Pulverized coal			No. 6 fuel oil		
Run designation	CM 1	CM 2	CM 3	PC 1	PC 2	PC 3	01	02	03
Thermal input MW	0.443	0.432	0.416	0.456	0.469	0.483	0.458	0.458	0.460
Atomizer type	Internal twin fluid			Pipe injector			External twin fluid		
Atomizing air/fuel ratio (kg/kg)	0.60	0.68	0.89	8.53	8.82	8.98	1.76	1.12	1.10
Atomizing air pressure (kPa)	467	494	536	near ambient	near ambient	near ambient	343	246	253
Total air (m3/kg fuel)	6.9	7.4	7.8	9.8	10.7	11.6	11.8	12.9	14.0
Temp °C of combustion air	70	64	61	59	61	53.0	64	61	57
Flue									
O_2 %	0.9	2.9	4.9	0.9	2.95	5.1	0.9	3.0	4.8
CO ppm	117	102	100	151	227	91	62.5	46.0	18.0
CO_2 %	16.2	15.0	13.7	17.0	15.2	13.2	14.8	13.1	12.0
N_2 %	82.9	82.1	81.4	82.1	81.9	81.7	84.3	83.9	83.2
NO_x ppm	454	582	457	698	776	688	343	340	323
SO_2 ppm	852	734	654	886	710	658	1358	1463	1042
SO_3 ppm	0.4	-	-	0.8	-	-	-	0.1	0.7
T_{flue} °C	434	513	479	459	579	546	536	551	571
P' gm/m^3	7.38	3.03	3.29	6.42	2.39	2.24	0.181	0.160	0.036
Carbon (1 - a') %	90.4	73.5	79.1	77.3	44.0	62.0	100	100	100
Cx %	84.0	95.3	93.6	90.2	97.7	95.3	99.7	99.8	99.9

All volume flowrates at 15.5°C and 101.3 kPa

P'; flue particulate loading

Table 2 - Fuel analysis coal-water fuel and Devco Lingan pulverized coal

	CWF	Pulverized coal		
Specific gravity at 20°C	1.16	-		
Moisture wt %	29.8, 31.1 and 32.4	0.35 - 0.74		
Apparent viscosity Pa.s (20°C) Shear rate s^{-1}	Thixotropic fluid	-		
154	0.971 (0.459)	-		
452	0.842 (0.514)	-		
Coal free swelling index	7	7		
Gross calorific value (dry) MJ/kg	37.67	34.9		
Proximate analysis (dry)				
Volatiles wt %	35.73	36.88		
Fixed carbon	62.6	60.32		
Ash	1.67	2.80		
Ultimate analysis (dry)				
C wt %	84.24	83.48		
H	5.47	5.32		
S	0.99	1.27		
N	1.93	1.79		
O	5.7	5.34		
Size distribution; μm, cum wt %		PC1	PC2	PC3*
>75	14.0	1.0	2.4	11.0
>64	20.0	3.2	7.0	19.0
>40.3	45.0	21.5	29.0	47.0
>25.4	65.0	61.0	55.0	70.0
>16	81.0	74.0	79.0	87.5
>10.1	92.5	92.5	93.0	96.5
> 5.1	99.6	100.0	100.0	100.0

*see Table 1

Table 3 - No. 6 fuel oil analysis

Specific gravity 15.5°C	0.986
A.P.I. at 15.5°C	12.01
Pour point (°C)	5.0
Flash point (°C)	102
viscosity in Pa.s	
at 40°C	1.080
54°C	0.355
70°C	0.146
100°C	0.039
Gross calorific value MJ/kg (Btu/lb)	42.48 (18265)
Ultimate analysis, wt %	
C	85.6
H	10.4
N	0.37
S	2.46
Ash	trace

Table 4 - Furnace operating conditions for swirling jet No. 6 oil and CWF flames

Fuel	No. 6 oil		Coal water fuel	
Type of atomizing medium	Air	Steam	Air	Steam
Thermal input MW	1.8	1.8	1.8	1.8
Atomizer type	NRCC 60°	Cone	NRCC 50°	Cone
Atomizing medium fuel ratio (kg/kg)	0.42	0.41	0.33	0.23
Atomizing medium pressure (KPa)	721	722	754	696
Combustion air (m^3/kg fuel)	15.77	16.28	9.70	9.50
Temp. of combustion air (°C)	237	253	253	254
Combustion air oxygen (%)	19.6	19.6	19.6	19.6
Flue				
O_2 %	5.02	5.51	4.93	4.90
CO_2 %	12.25	11.65	13.60	13.80
CO %	0.003	0.002	0.005	0.004
NO_x %	0.032	0.028	0.061	0.062
SO_2 %	0.130	0.119	0.063	0.065
T_{flue} °C	1004	998	1052	1037
P' gm/m^3	5.88	4.81	9.16	5.52
ash % (dry)	1.6	Insufficient	26.75	38.70
C_x %	98.77	sample	95.91	97.64
Carbon burnout % (from CO_2)	100	98.36	97.54	98.79

All volume flows at 15°C; 101.3 KPa

P'; flue particulate loading

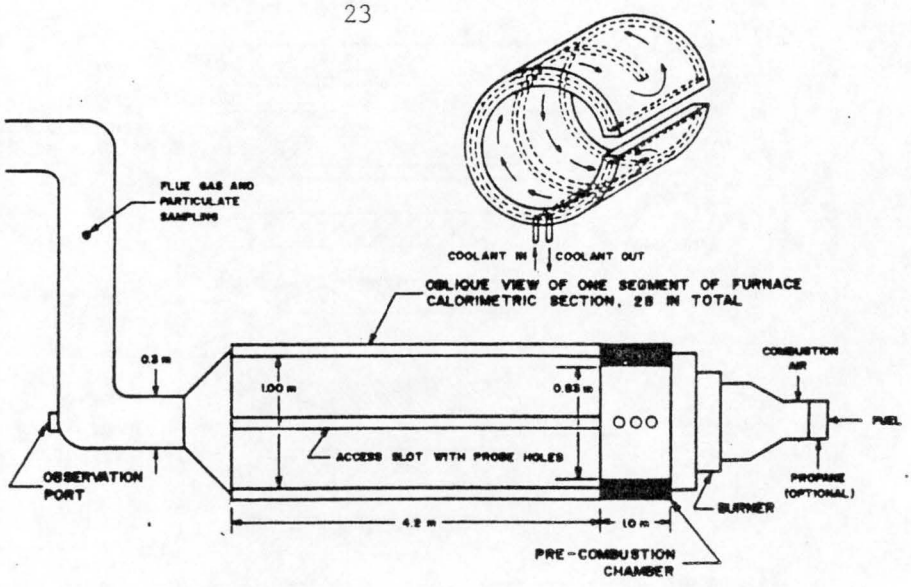

Fig. 1 - The ERL flame tunnel furnace

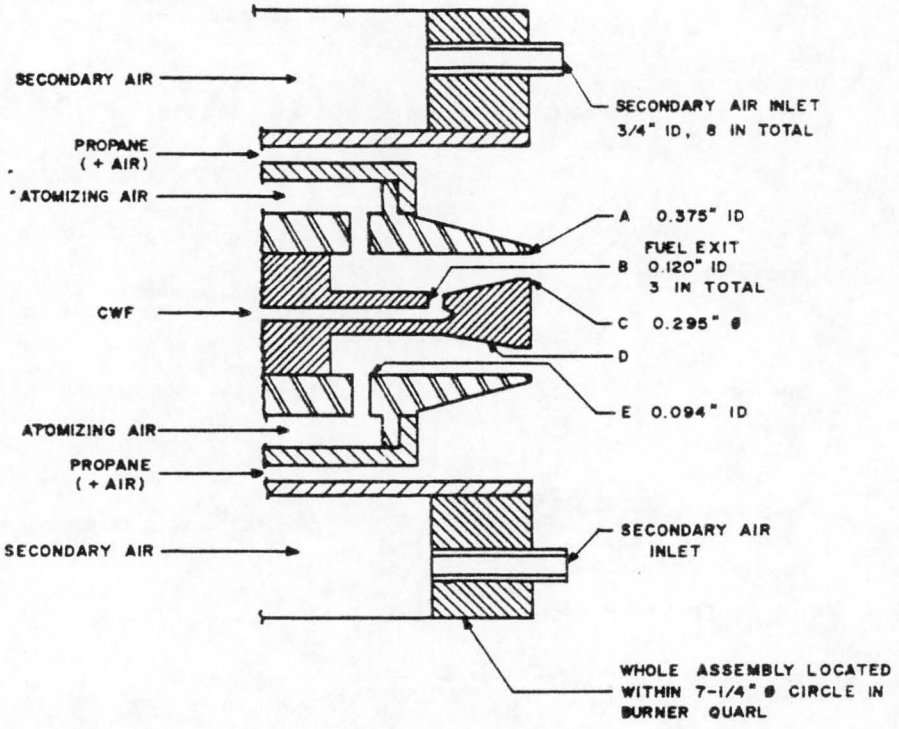

N.B. PREMIXED PROPANE SUPPORT FLAME FOR INITIAL IGNITION ONLY.

SUMMARY OF NOZZLE WEAR

RUN	A	B	C	D	E
CWF 5% O_2	0.386"-0.394"	0.120"	0.292"	PARTICLE TRACKS WITH SURF. WEAR	0.094"
CWF 3% O_2	0.383"-0.395"	0.127"-0.128"	0.293"	"	0.094"
CWF 1% O_2	0.386"-0.405"	0.128"-0.129"	0.293"	"	0.094"

Fig. 2 - Internally mixed CWF nozzle

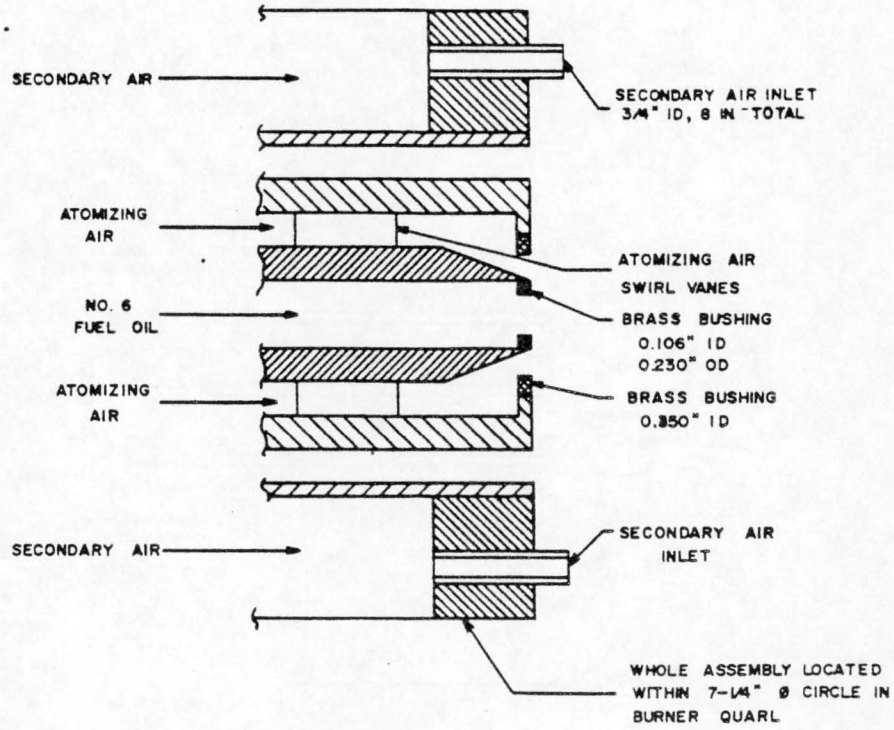

Fig. 3 - Externally mixed No. 6 oil nozzle

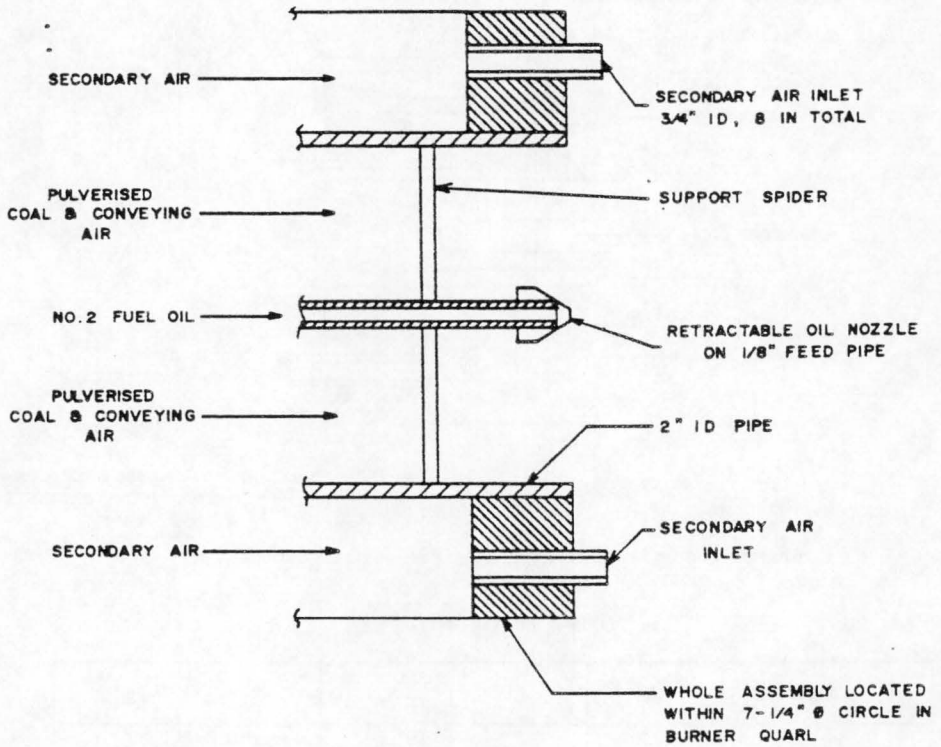

N.B. OIL GUN IN POSITION DURING FURNACE WARM-UP AND DURING INITIAL IGNITION OF PULVERISED COAL

Fig. 4 - Pulverized coal injector

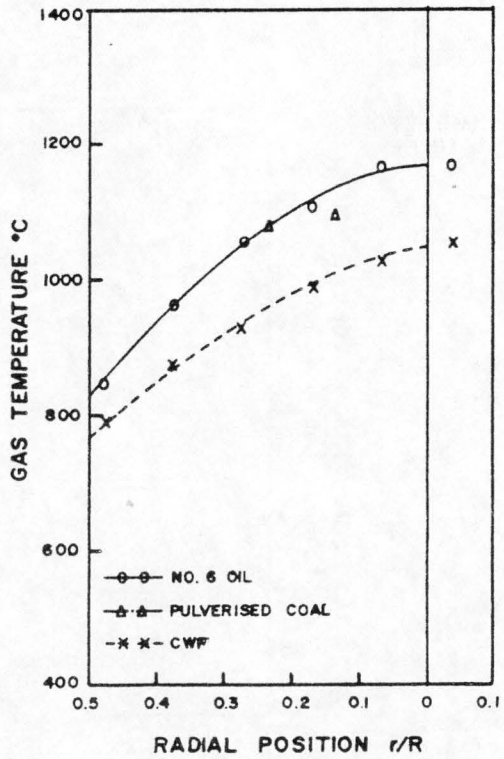

Fig. 5 - Radial gas temperatures; 1% O_2, 1.87 m

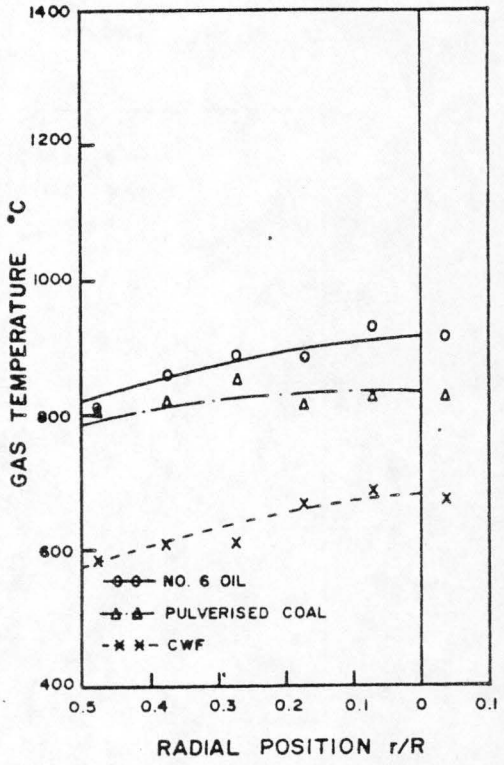

Fig. 6 - Radial gas temperatures; 1% O_2, 2.92 m

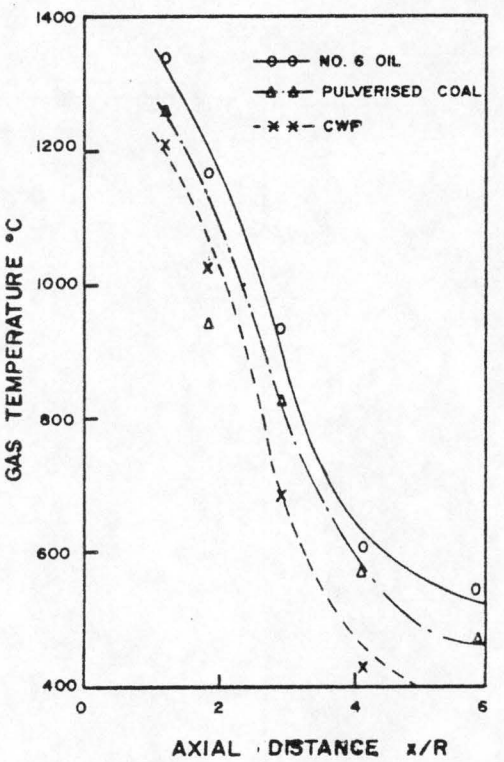

Fig. 7 - Peak centre line gas temperatures

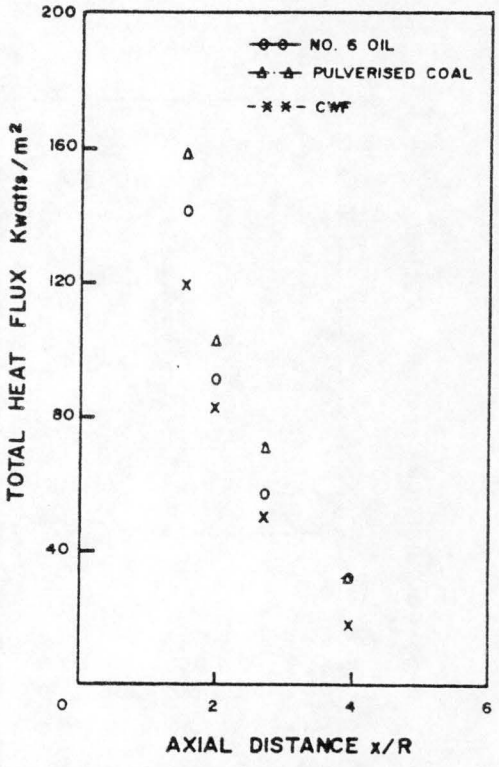

Fig. 8 - Total heat flux; 1% O_2

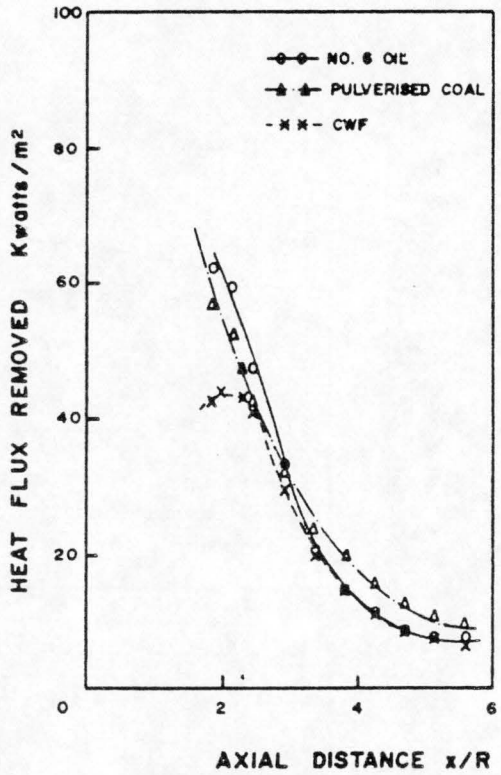

Fig. 9 - Cooling load heat flux; 1% O_2,

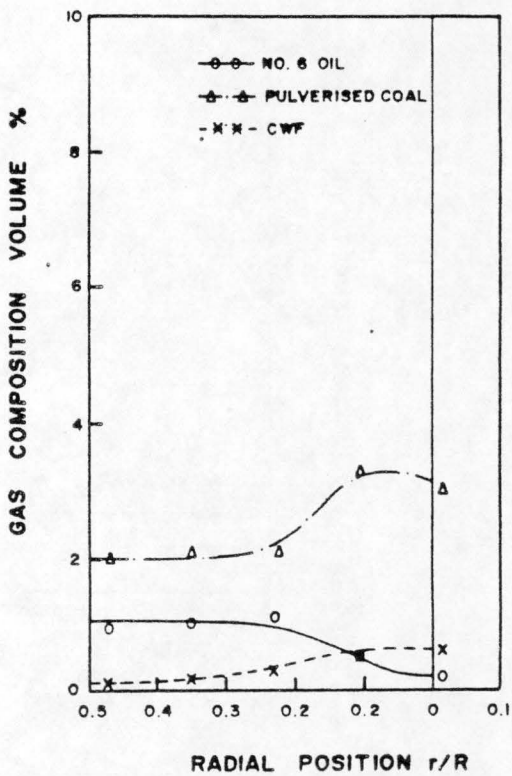

Fig. 10 - Oxygen concentration; 1% O_2, 1.26 m

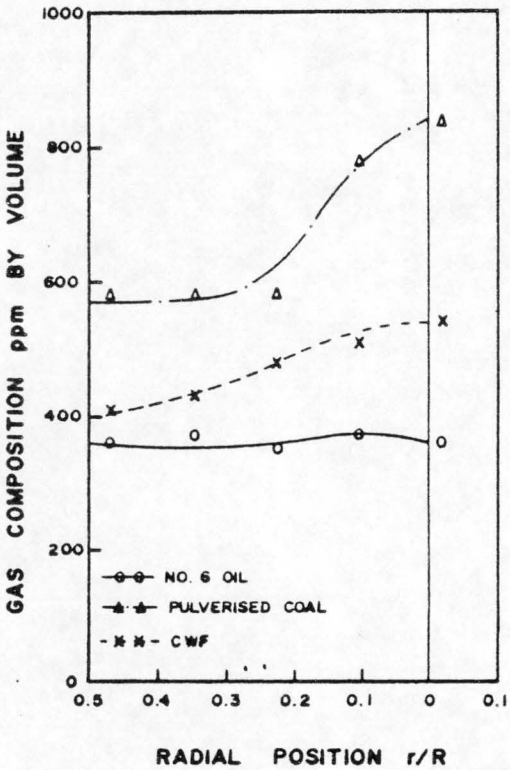

Fig. 11 - NO_x concentration; 1% O_2, 1.26 m

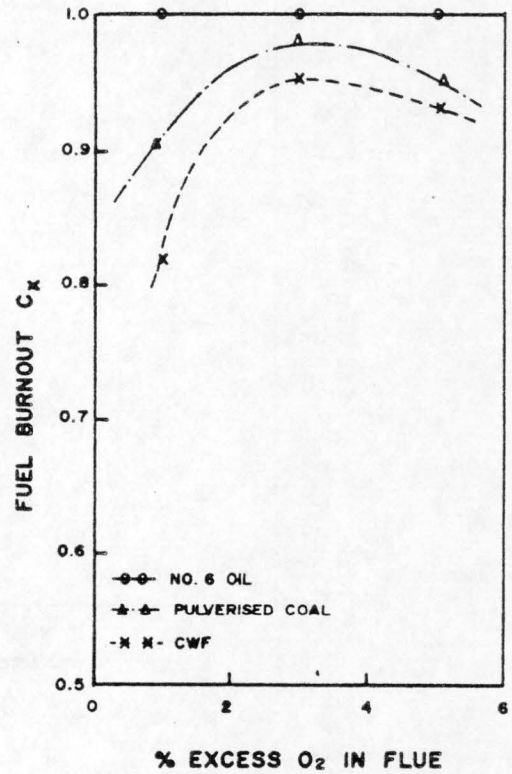

Fig. 12 - Fuel burnout efficiencies

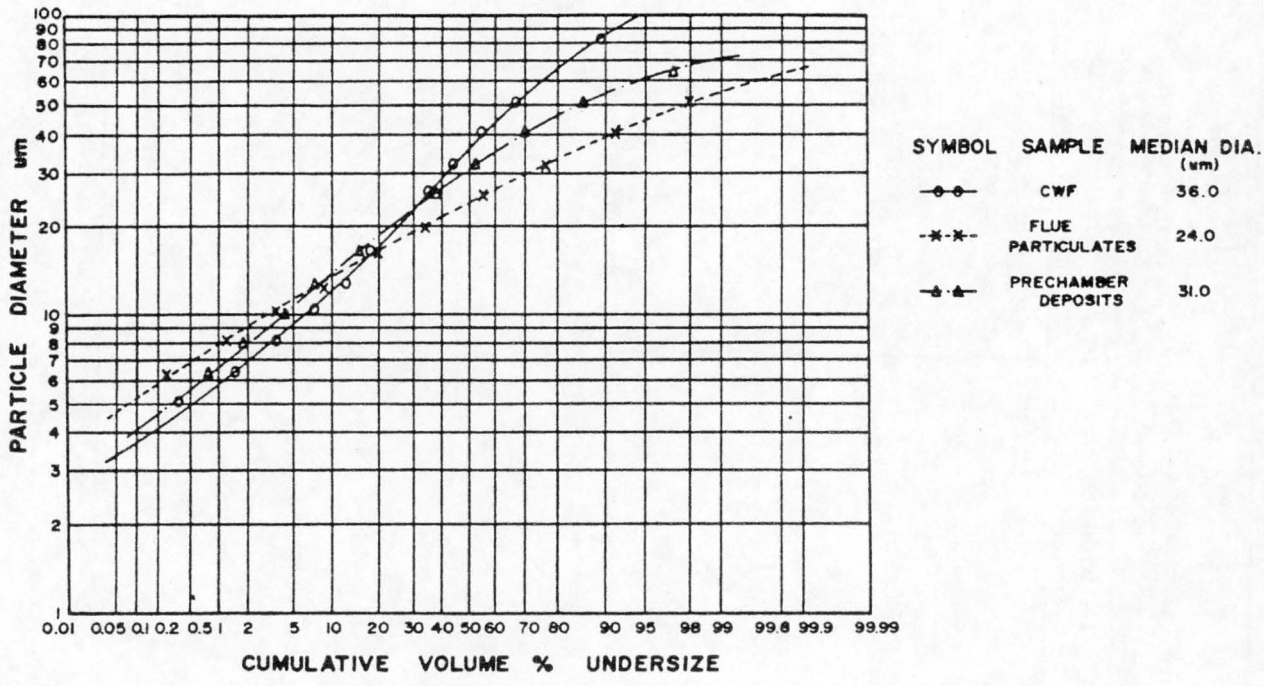

Fig. 13 - Size distribution in CWF, flue particulates and furnace deposits; 1% O_2

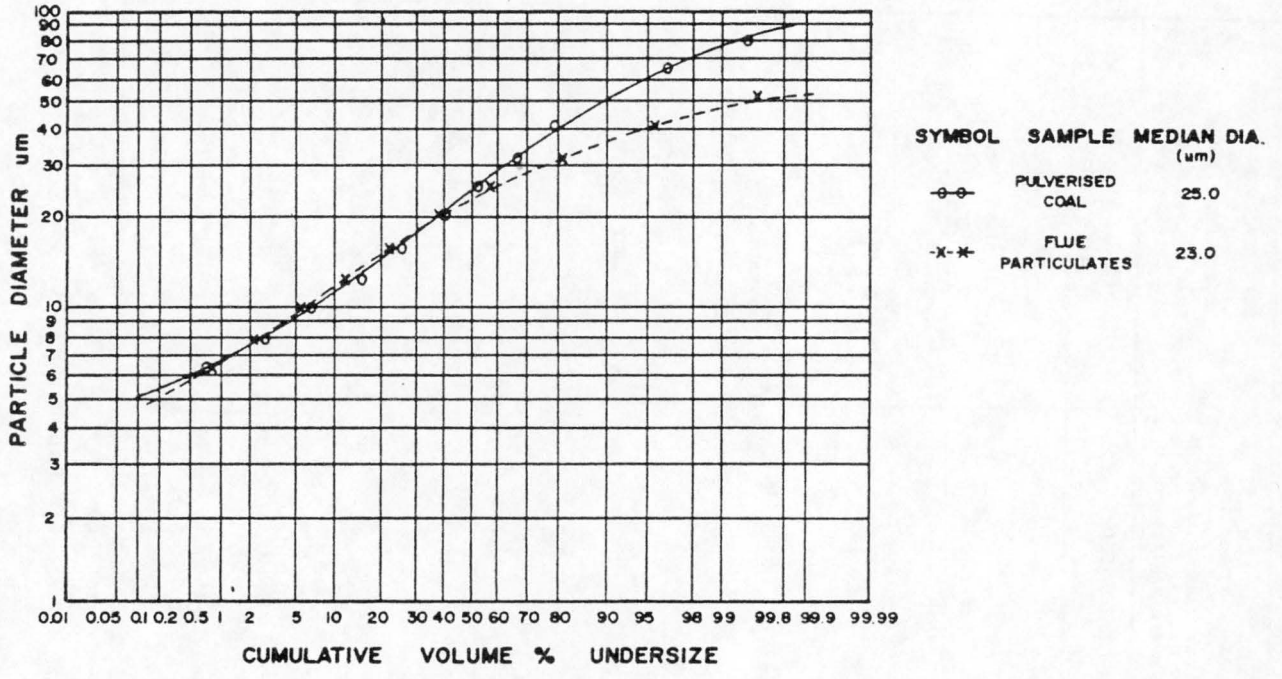

Fig. 14 - Size distribution in pulverized coal and flue particulates; 1% O_2

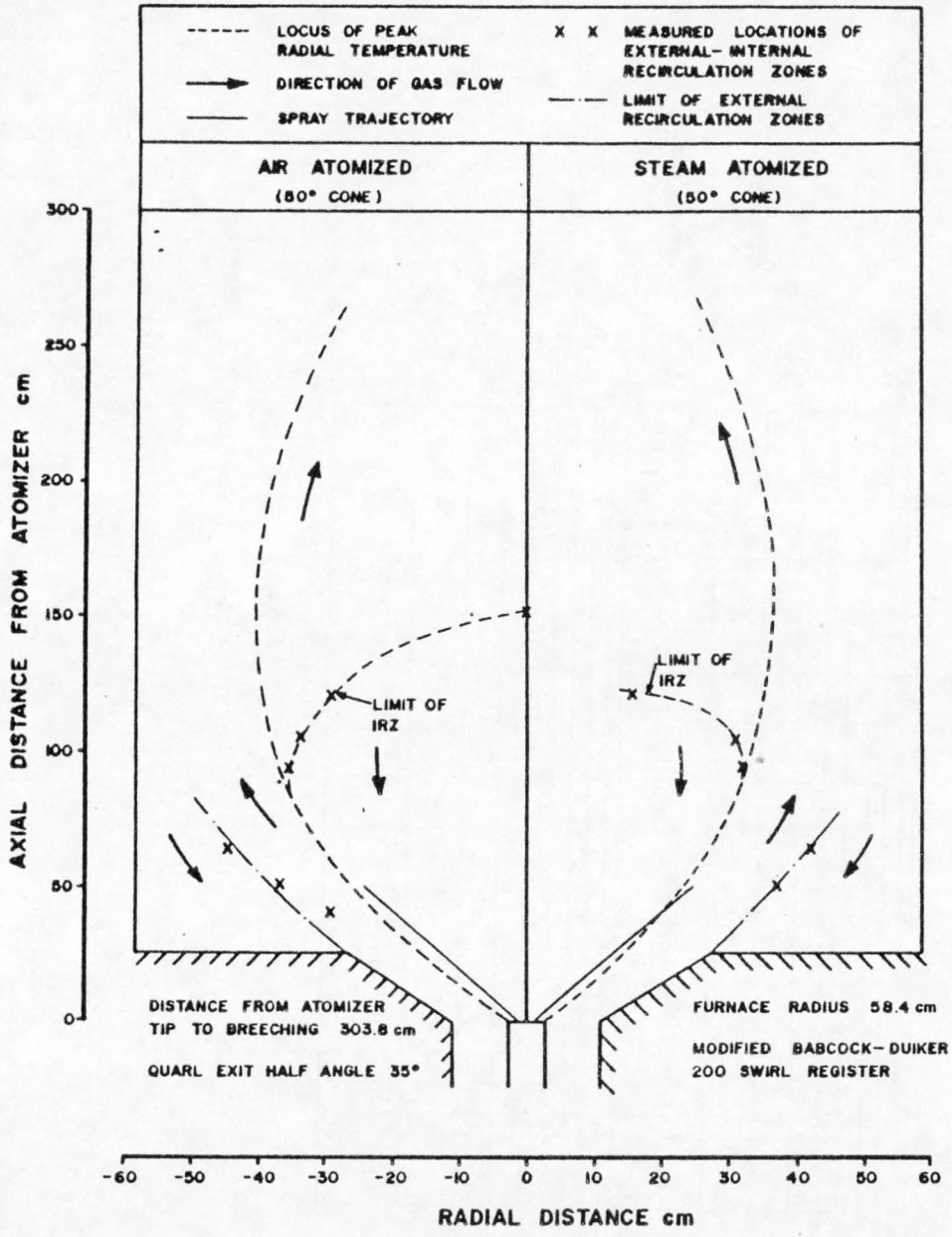

Fig. 15 - CWF flame flow boundaries; 1.8 MW_{th}, 5% O_2

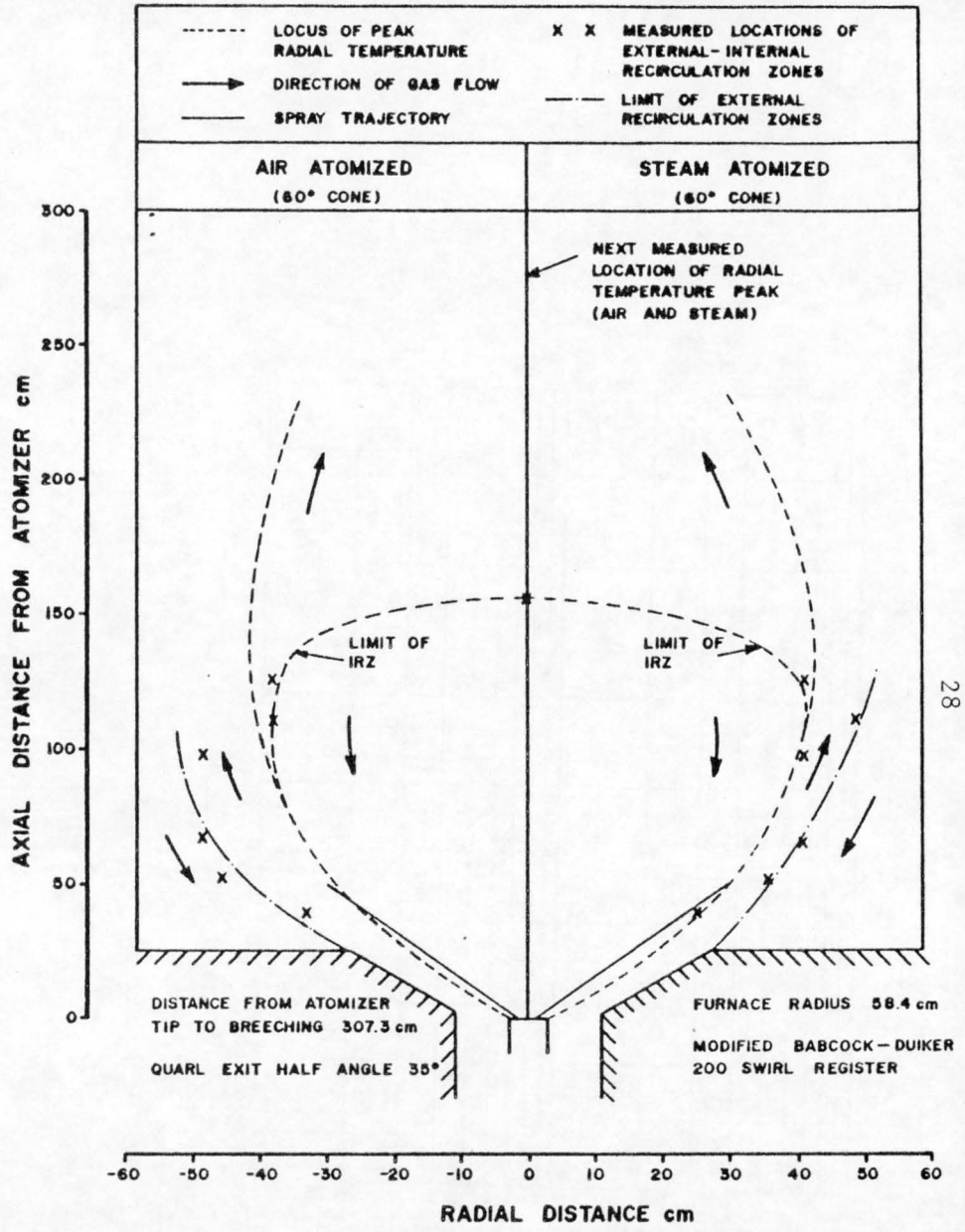

Fig. 16 - No. 6 oil flame flow boundaries; 1.8 MW_{th}, 5% O_2

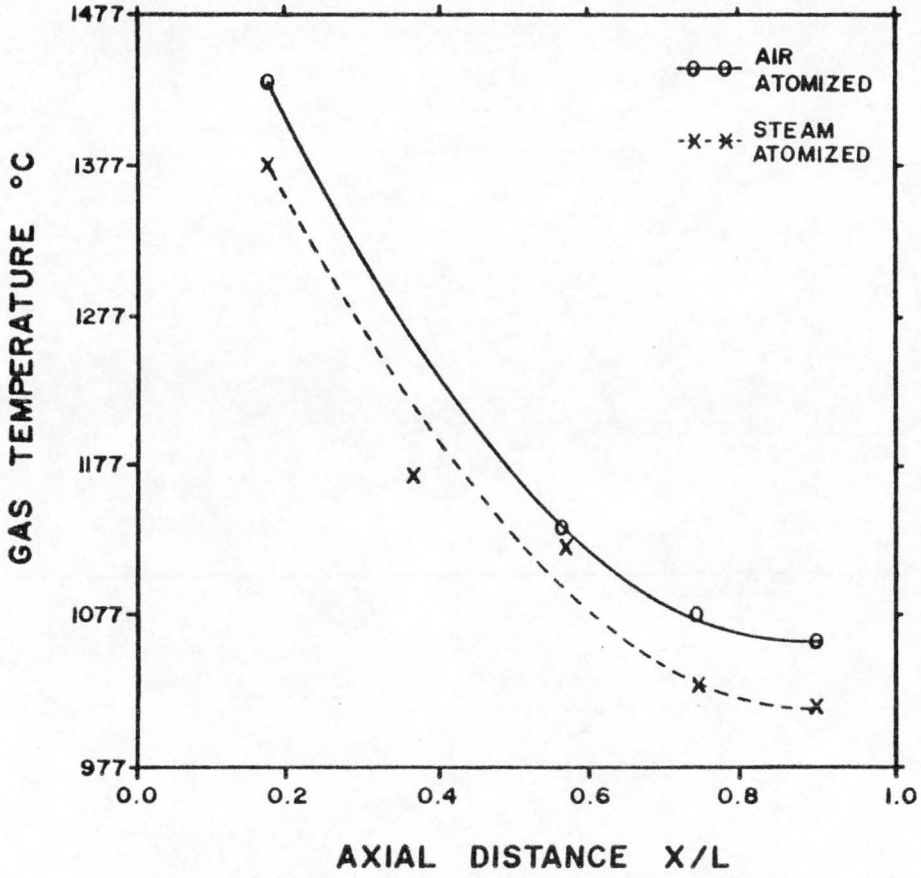

Fig. 17 - No. 6 oil centre line temperatures; 1.8 MW_{th}, 5% O_2

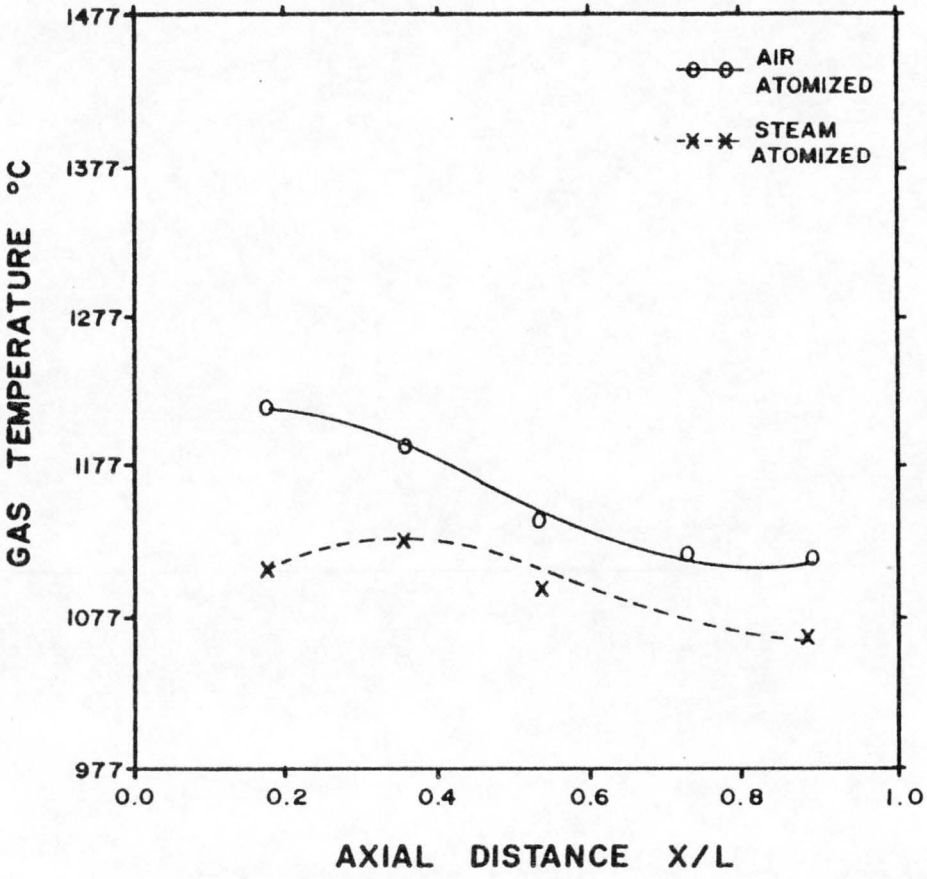

Fig. 18 - CWF centre line temperatures; 1.8 MW_{th}, 5% O_2